Quantum Mechanics/Molecular Mechanics (QM/MM) Study on Caspase-2

Recognition by Peptide Inhibitors

Petar M. Mitrasinovic*

- 4 Center for Biophysical and Chemical Research, Belgrade Institute of Science and Technology,
- 5 11060 Belgrade, Serbia; *E-mail: pmitrasinovic.ist-belgrade.edu.rs@tech-center.com

Abstract

1

2

6

7

8

9

1011

12

1314

15

16

17

18

19

20

21

22

2324

25

26

27

For a variety of biological and medical reasons, ongoing development of humane caspase-2 inhibitors is of vital importance. Herein, a hybrid two-layered QM/MM molecular model is derived in order to better understand the affinity and specificity of peptide inhibitors that interact with caspase-2. By taking care of both the unique structural features and the catalytic activity of human caspase-2, the critical residues (E217, R378, N379, T380, and Y420) of the enzyme with the peptide inhibitor are treated at QM level (the Self-Consistent-Charge Density-Functional Tight-Binding method with the Dispersion correction (SCC-DFTB-D)), while the remaining part of the complex is treated at MM level (AMBER force field). The QM/MM binding free energies (BFEs) are well-correlated with the experimental observations and indicate that caspase-2 uniquely prefers a penta-peptide such as VDVAD. The sequence of VDVAD is varied in a systematic fashion by considering the physicochemical properties of every constitutive amino acid and its substituent, and the corresponding BFE with the inhibition constant (K_i) is evaluated. The values of K_i for several caspase-2:peptide complexes are found to be within the experimental range (between 0.01 nM and 1 μ M). The affinity order is: VELAD (K=0.081 nM) > VDVAD $(K_i=0.23 \text{ nM}) > \text{VEIAD} (K_i=0.61 \text{ nM}) > \text{VEVAD} (K_i=3.7 \text{ nM}) > \text{VDIAD} (K_i=4.5 \text{ nM}) \text{ etc. An}$ approximate condition needed to be satisfied by the kinetic parameters (the Michaelis constant - $K_{\rm M}$ and the specificity constant - $k_{\rm cat}/K_{\rm M}$) for competitive inhibition is reported. VELAD and VDVAD are suggested to be most specific to caspase-2 and both are nearly 1.5, 3 and 4 times more specific to the receptor than VEIAD, VEVAD and VDIAD respectively. Additional kinetic threshold, indicating which peptides may be treated as tightly bound inhibitors, is given.

Key words: enzyme, human caspase-2, inhibition, peptide inhibitor, QM/MM, SCC-DFTB-D

1. Introduction

2930

31

32

33

34

35

3637

38

39

40

41

42

43

4445

46

47

48

49

50

5152

53

54

55

56

57

58 59 Homologues that make up the caspase (casp) family of cysteine proteases are essential mediators of cellular processes, such as apoptosis, proliferation, and differentiation. They are synthesized and stored as inactive zymogens, as well as divided into inflammatory (caspase-1, -4, -5, -12 in humans and caspase-1, -11, and -12 in mice) and apoptotic (caspase-3, -6, -7, -8, and -9 in mammals) caspases according to their function and pro-domain structure. The functions of caspase-2, -10, and -14 can not be easily categorized. Apoptotic caspases are further subclassified by their mechanism of action as initiators (caspase-8 and -9) and executioners (caspase-3, -6, and -7).

The first identified mammalian member is caspase-2 and its physiological role is not quite clear. Caspase-2, one of the most evolutionarily conserved caspases, is inclined to behave as either executioner or initiator. In terms of substrate specificity, caspase-2 is similar to caspase-3 and -7 (executioner caspases). However, the long N-terminal caspase recruitment domain (CARD) of caspase-2 indicates its potential role as an initiator caspase.³ While the function of caspase-2 in the embryonic development of mice is questionable.⁴ its important role in stressinduced cell death pathways and tumor suppression is more certain.⁵ The potential roles of caspase-2 in mediating nonapoptotic pathways (cell-cycle regulation and DNA repair) have been reported in terms of whether caspase-2 is mandatory for apoptosis under specific circumstances, 6,7 or whether it primarily functions in cell-cycle regulation. 5 An elevated expression level of caspase-2 has been observed in the brain of patients with some neurodegenerative disorders.⁸ In addition, the critical role of caspase-2 in mediating nonalcoholic steatohepatitis (NASH) pathogenesis, a chronic and aggressive liver condition not only in mice but probably in humans, has been highlighted. Whereas many questions on caspase-2 physiology remain enigmatic, one of the key aspects for developing caspase-2 specific probes is related to the way in which caspase-2 gets activated.

Peptide bonds are hydrolyzed using caspases (endoproteases) in a reaction that depends on catalytic cysteine residues in the caspase active site and occurs only after certain aspartic acid residues in the substrate. Besides resulting in substrate inactivation, caspase-mediated processing may generate active signaling molecules that participate in apoptosis and inflammation. Caspase activities are strictly regulated by protein-protein interactions and by proteolysis. The crystal structures of caspase-2 in complex with several peptide inhibitors and comparison of the apo

(substrate-free) and inhibited caspase-2 structures have revealed a recognition via several discrete catalytic steps: (i) activation of caspase-2 by breaking a nonconserved salt bridge between Glu217 (caspase-2 is the only human caspase with glutamate at position 217) and the invariant Arg378, (ii) formation of a catalytically competent conformation upon binding to a single substrate, and (iii) formation of the enzyme-substrate complex after having both active sites occupied by the substrate. Caspase-2 has been suggested to uniquely prefer a pentapeptide rather than a tetra-peptide, as required for efficient cleavage by other caspases. To gain more complete insights into the caspase-2/peptide recognition and further facilitate the design of caspase-2 inhibitors, a hybrid QM/MM approach is employed in this work.

2. Methods

To obtain the initial atomic coordinates of the apo and inhibited caspase-2 structures, the experimental structures were retrieved from the Research Collaboratory for Structural Bioinformatics (RCSB) Protein Data Bank (PDB): 3R7S.PDB (apo caspase-2), 3R6G.PDB (caspase-2/VDVAD), 3R5J.PDB (caspase-2/ADVAD), 3R7B.PDB (caspase-2/DVAD), and 3R6L.PDB (T380A/VDVAD). The sequence of the penta-peptide inhibitor was varied using single point mutations generated by applying the Mutagenesis engine of PyMol-v0.99 to the experimental structure 3R6G.PDB in a backbone-dependent fashion. 11

Before running QM/MM calculations, the systems were prepared using the Amber 11 suite of programs. ^{12,13} The solute was prepared using the Amber11 utility program tLeap in association with the ff99sb force field. ¹⁴ Every inhibitor was initially prepared by parameteryzing its atom types, charges, and connectivity in order to be treated as part of the solute. The molecular geometry was optimized by Gaussian 98 at the MP2/6-31G* level of theory. ¹⁵ The molecular electrostatic potential was calculated by Gaussian 98 at the HF/6-31G* level of theory, ¹⁵ while the atomic charges were derived by means of the RESP fitting technique, ¹⁶ which is part of AmberTools 1.5. ^{12,13} Remaining parameters were assigned from the General Amber Force Field (GAFF), ¹⁷ being entirely compatible with the ff99sb macromolecular force field. ¹⁴ Every solute was solvated using a 10 Å (1 Å=10⁻¹⁰ m) pad of TIP3P water molecules (≈ 11500) and the counter ions Na⁺ were added to neutralize each system. To remove clashes and bad contacts, two-stage geometric minimization was performed using the Sander module of Amber11. ^{12,13} At the outset, the positions of the solute atoms were kept fixed, while the positions of the water atoms were minimized by gradually reducing an initial harmonic

restraint of 2 kcal mol⁻¹ Å⁻² on all non-hydrogen non-water atoms via 5000 combined steepest descent (2500 steps) and conjugate gradient (2500 steps) minimization steps. Afterwards, the entire system was minimized without restrains by means of 10000 combined steepest descent (5000 steps) and conjugate gradient (5000 steps) minimization steps.



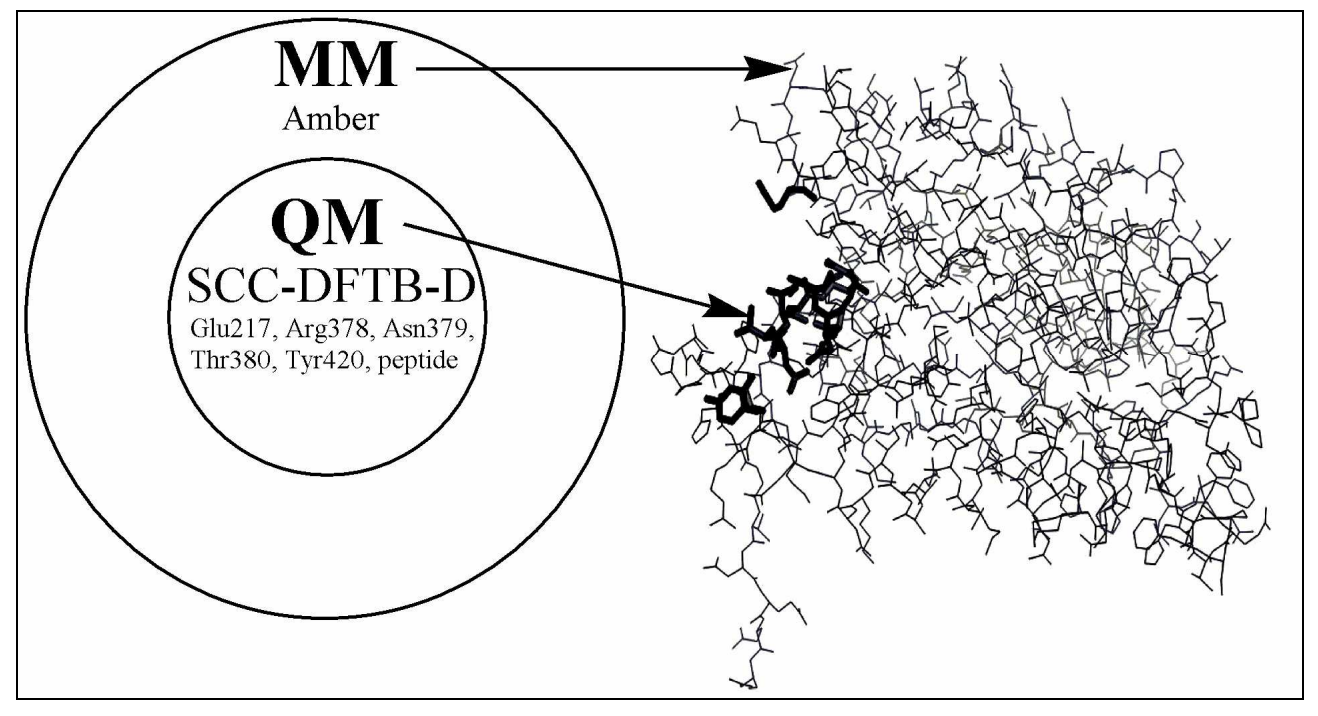


Figure 1. The two-layered QM/MM (SCC-DFTB-D/AMBER) model was used to evaluate the efficacy of peptide inhibitors towards caspase-2.

A two-layered hybrid approach was employed to assess the binding affinities within the caspase-2:peptide complexes. The outer layer of the complex (Figure 1) was kept at the low level of theory (MM) with an Amber force field. The central layer of the complex (bold sticks; Figure 1) was treated at the high level of theory (QM), employing SCC-DFTB-D, the Self-Consistent-Charge Density-Functional Tight-Binding method ^{18,19} with Dispersion energy, ²⁰ as implemented in Amber11. ^{21,22} The inclusion of the empirical correction for dispersion energy into SCC-DFTB provided a balanced and reliable description of the interactions inside the systems. ²³ Pure Density Functional Theory (DFT) methods are known for their modest computational costs, but they are not able to adequately describe dispersive forces, especially within unconventional systems, ^{24,25} as many density functionals are empirical. ²⁰ DFT was extended to include dispersion correction (DFT-D), ^{26,27} and as such DFT-D became suitable for performing energy

minimizations and vibrational analyses of extended molecular complexes containing hundreds of atoms. By being a few orders of magnitude faster than DFT-D,^{23,28-33} SCC-DFTB-D was suggested to be applicable to both quantumchemical simulations and calculations pertaining to a large number of extended molecular complexes.²³

The total interaction energies were defined as:

116
$$\Delta E_{\text{interaction}} = \Delta E_{\text{model,high}} + \Delta E_{\text{real,low}} - \Delta E_{\text{model,low}}$$
 (1)

- where ΔE_{model} denote the energies of the model system defined at high and low level of theory
- and ΔE_{real} denote the whole (real) system. Therefore, the equivalent binding free energies of the
- 119 complex systems were determined as:

120
$$\Delta G_{\text{binding}} \approx \Delta G = G_{\text{casp-2:peptide}} - [G_{\text{casp-2}} + G_{\text{peptide}}]$$
 (2)

- The thermodynamic quantities (enthalpies, entropies, and different entropic contributions) were
- obtained from frequency calculations done by the Nmode module of Amber 11. 12,13 The different
- entropic contributions (translation, rotation, and vibration) for caspase-2:peptide complexes were
- 124 calculated as:

126

127128

129

130

131

132

133

134

135

136

137

138

139

125
$$\Delta S = S_{\text{casp-2:peptide}} - [S_{\text{casp-2}} + S_{\text{peptide}}]$$
 (3)

3. Results and Discussion

Kinetic measurements of competitive inhibition associated with the initial experimental structures¹⁰ are summarized in Table 1. The specificity constant (k_{cat}/K_M) identified the pentapeptide VDVAD as a preferred inhibitor, while two residues, Thr380 and Tyr420, were identified as critical for recognizing a residue at the P5 position - the first position at the left end in the peptide sequence (Figures 2b & 2c). The salt bridge between Glu217 and Arg378, which is present in the apo caspase-2 (3.37 Å, Figure 2a), is broken in the caspase-2:VDVAD complex (8.05 Å, Figure 2b), because Thr380 and Tyr420 in P5 recognition move 2.1 and 3.6 Å, respectively (Figure 2d). Furthermore, the specificity constant revealed that mutation of Thr380 to Ala reduces the catalytic efficiency of caspase-2 by about 40 fold (Table 1), as Thr380Ala (Figure 2c) causes the loss of the hydrogen bond between Thr380 and the P5 side chain (3.51 Å, Figure 2b) due to a 2.3 Å movement in the main chain in residue 380. Structurally speaking in a similar manner, mutation of Tyr420 to Ala reduces the catalytic efficiency of caspase-2 by about

4 fold (Table 1), as Tyr420Ala causes a 0.5 Å movement of the side chain of residue 420 and the
 loss of the hydrophobic interaction between Tyr420 and the P5 side chain.

Table 1. Kinetic data¹⁰ for experimental caspase-2:peptide inhibitor complexes: $K_{\rm M}$ - Michaelis constant, $k_{\rm cat}$ - catalytic constant, $k_{\rm cat}/K_{\rm M}$ - specificity constant, and IC_{50} - inhibitory concentration

Complex ^(a)	$K_{\mathrm{M}}^{\mathrm{(b)}}$	k _{cat}	$k_{ m cat}/K_{ m M}$	<i>IC</i> ₅₀ ^{(b),(c)}
PDB ID	(μΜ)	(s ⁻¹)	$(\mu M^{-1} s^{-1})$	(nM)
wt:VDVAD	25	0.60	0.024	25
3R6G				
wt:ADVAD	150	0.81	0.0055	110
3R5J				
wt:DVAD	92	0.12	0.0013	710
3R7B				
Y420A:VDVAD	84	0.52	0.0062	314
3R6G				
T380A:VDVAD	220	0.13	0.00060	347
3R6L				
T380A/Y420A:VDVAD	> 400	< 0.000014	N/A	574
3R6L				

^{144 (}a) wild-type (wt) casp-2, Ala (A), Asp (D), Thr (T), Tyr (Y), Val (V)

 $^{145 \}qquad {}^{\text{(b)}} \ 1 \ \mu M = 10^{\text{-6}} \ M, \ 1 \ nM = 10^{\text{-9}} \ M$

^{146 (}c) *IC*₅₀ represents the concentration at which a substance exerts half of its maximal inhibitory effect.

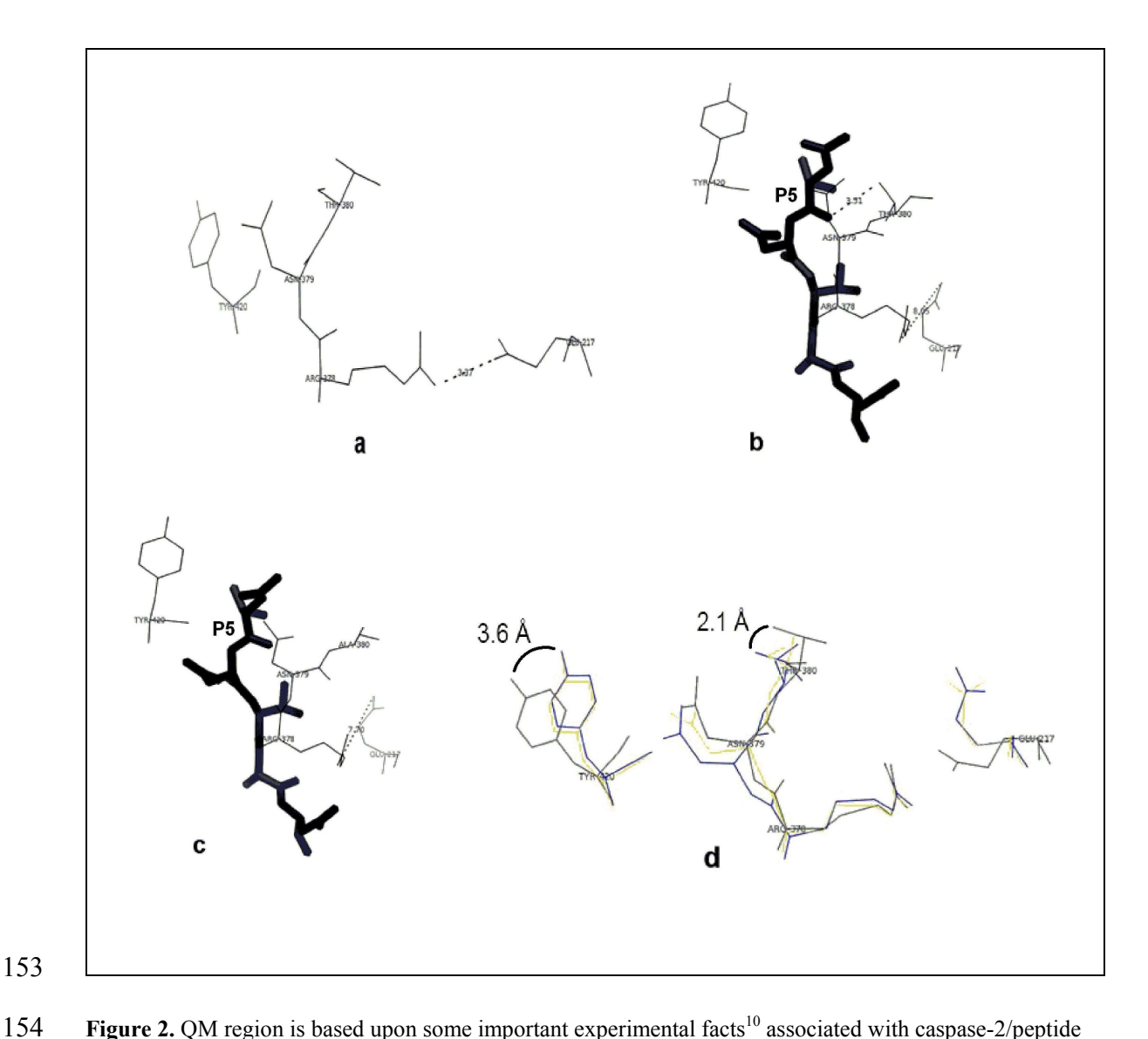


Figure 2. QM region is based upon some important experimental facts¹⁰ associated with caspase-2/peptide recognition: (**a**) apo (ligand-free) caspase-2 with Glu217-Arg378 salt bridge (3.37 Å), (**b**) caspase-2:VDVAD without Glu217-Arg378 (8.05 Å) salt bridge, (**c**) Thr380Ala:VDVAD without Glu217-Arg378 (7.70 Å) salt bridge, and (**d**) overlay of enzyme residues of apo caspase-2 (black), caspase-2:VDVAD (blue), and Thr380Ala:VDVAD (yellow). VDVAD is denoted by bold sticks in (**b**) and (**c**), P5 - the first position at the left end in the peptide sequence.

To perform physically realistic QM/MM calculations, the first important aspect is how to define a QM region, or what caspase-2 residues need to be included in the QM region. There are no good universal rules here. Binding site residues of caspase-2 that are involved in noncovalent interactions with a peptide inhibitor are: Arg219, His277, Gly278, Gln318, Cys320, Ala376, Arg378, Asn379, Thr380, Trp385, Arg417, Glu418, and Tyr420. Caspase-2 is the only human

caspase with glutamate at position 217 forming a salt bridge with Arg378 in the apo caspase-2 (Figure 2a). The inhibition of caspase-2 was related to breaking the Glu217-Arg378 salt bridge, while residues Thr380 and Tyr420 were pointed out as the key elements for recognizing a preferred penta-peptide along a catalytic pathway (Figure 2b). An intention to define a QM region to mimic the active site has to take into account all these experimental and structural arguments. Knowing that inclusion of a different number of caspase-2 residues in the QM region is associated with different thermodynamic properties such as the binding free energies means that an appropriate QM region is supposed to generate results in agreement with experimental data. Even though one might want to have as large a QM region as possible, having more than 80-100 atoms in a QM region lead to simulations that are computationally very expensive. To reconcile all the structural, functional, and computational standpoints as much as possible, the present choice of including Glu217, Arg378, Asn379, Thr380, Tyr420, and the peptide inhibitor in the QM region (Figure 1) is carefully made in order to generate the inhibition constants that are within an experimental range – from 1 μ M (1 μ M = 10⁻⁶ M) to 0.01 nM (1 nM = 10⁻⁹ M) for inhibited caspase-2 structures.

Table 2. Binding free energies that are evaluated using QM/MM (SCC-DFTB-D/AMBER) method for experimental caspase-2:peptide structures

Complex ^(a)	$\Delta G_{ m bind}^{ m (b)}$	ΔH	$T\Delta S_{ m total}$	$T\Delta S_{\mathrm{trans}}$	$T\Delta S_{ m rot}$	$T\Delta S_{ m vib}$
PDB ID	(kcal mol ⁻¹)	(kcal mol ⁻¹)	(kcal mol ⁻¹)	(kcal mol ⁻¹)	(kcal mol ⁻¹)	(kcal mol ⁻¹)
wt:VDVAD	-13.22	-31.85	-18.63	-12.90	-10.61	4.88
3R6G						
wt:ADVAD	-9.83	-30.35	-20.52	-12.87	-10.56	2.91
3R5J						
Y420A:VDVAD	-9.17	-30.29	-21.12	-12.87	-10.38	2.13
3R6G						
T380A:VDVAD	-8.71	-29.74	-21.03	-12.90	-10.80	2.67
3R6L						
T380A/Y420A:VDVAD	-5.53	-25.69	-20.16	-12.81	-10.53	3.18
3R6L						
wt:DVAD	-2.75	-24.28	-21.53	-12.81	-10.58	1.86
3R7B						

⁽a) wild-type (wt) casp-2, Ala (A), Asp (D), Thr (T), Tyr (Y), Val (V)

⁽b) Gibb's free energy (ΔG), enthalpy (ΔH), entropy ($T\Delta S$) and entropic contribution, translational ($T\Delta S_{trans}$), rotational ($T\Delta S_{rot}$), vibrational ($T\Delta S_{vib}$) are derived from Eqs. 2 and 3.

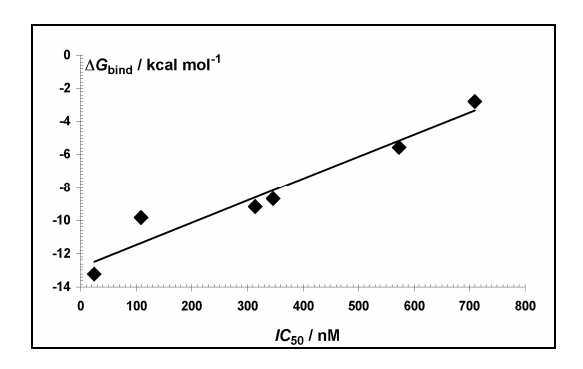


Figure 3. Correlation of the calculated binding free energy ($\Delta G_{\rm bind}$) with the measured inhibitory concentration (IC_{50}) for the experimental caspase-2:peptide structures. $\Delta G_{\rm bind} = 0.013 \ IC_{50}$ -12.85, R = 0.97.

QM/MM binding free energies for the experimental structures are given in Table 2. Figure 3 shows quite a satisfactory linear correlation between the calculated $\Delta G_{\rm bind}$ (Table 2) and the experimental inhibitory concentration IC_{50} (Table 1): $\Delta G_{\rm bind} = 0.013 \ IC_{50} -12.85$, R = 0.97. The most negative BFE for the caspase-2:VDVAD complex (-13.22 kcal mol⁻¹) signifies that

VDVAD is a favorable inhibitor. The enthalpy contribution (ΔH) for the complexes ranges from -31.85 to -24.28 kcal mol⁻¹, indicating that the noncovalent complexation process is exothermic. In case of the entropy contribution ($T\Delta S$), the less negative entropy change is, the more reduced degrees of freedom of an inhibitor in the protein active pocket are. The least negative entropy (-18.63 kcal mol⁻¹) is associated with caspase-2:VDVAD, of which vibrational contribution (4.88 kcal mol⁻¹) makes a most conspicuous difference with respect to the other complexes (Table 2). The increased and thermodynamically favorable vibrational entropy change upon binding of VDVAD to caspase-2 is the signature of preferred noncovalent complexation.

Table 3. QM/MM binding free energies that are within experimental range (between -8.23 and -15.09 kcal mol⁻¹) for caspase-2:peptide complexes

Complex ^(a)	$\Delta G_{ m bind}^{(b)}$	ΔH	$T\Delta S_{ ext{total}}$	$K_{i}^{(b)}$	
	(kcal mol ⁻¹)	(kcal mol ⁻¹)	(kcal mol ⁻¹)	(μΜ)	
casp-2:VELAD	-13.84	-33.49	-19.65	0.000081	
casp-2:VDVAD	-13.22	-31.85	-18.63	0.00023	
casp-2:VEIAD	-12.64	-30.91	-18.27	0.00061	
casp-2:VEVAD	-11.57	-29.60	-18.03	0.0037	
casp-2:VDIAD	-11.45	-32.75	21.30	0.0045	
casp-2:VDLAE	-11.09	-29.12	-18.03	0.0083	
casp-2:IEIAD	-10.85	-26.60	-15.75	0.012	
casp-2:IDVAD	-10.72	-29.35	-18.63	0.015	
casp-2:LDIAD	-10.54	-31.87	-21.33	0.021	
casp-2:VDLGE	-10.52	-28.82	-18.30	0.022	
casp-2:VEIGE	-10.21	-29.29	-19.08	0.036	
casp-2:IDLAD	-10.07	-29.96	-19.89	0.045	
casp-2:IEIGE	-10.01	-33.26	-23.25	0.050	
casp-2:IDIAD	-9.80	-29.63	-19.83	0.072	
casp-2:LELAD	-9.75	-32.91	-23.16	0.078	
casp-2:VELGE	-9.33	-28.38	-19.05	0.16	
casp-2:VDLAD	-9.27	-29.52	-20.25	0.17	
casp-2:LELAE	-8.55	-29.13	-20.58	0.59	

⁽a) Ala (A), Asp (D), Glu (E), Ile (I), Leu (L), Val (V)

⁽b) Gibb's free energy (ΔG), enthalpy (ΔH), entropy ($T\Delta S$), inhibition constant (K_i), $\Delta G_{bind} = RT \ln(K_i)$, R – the gas constant (1.9872 kcal K⁻¹ mol⁻¹), T – the absolute temperature (300 K), 1 μ M = 10⁻⁶ M

To search for more effective penta-peptides, the sequence of VDVAD is systematically varied by means of single point mutations of its constitutive residues. To make such a procedure consistent, each amino acid is mutated to its counterpart observed from a physicochemical standpoint. Val (V), an aliphatic and hydrophobic amino acid, is mutated to either Ile (I) or Leu (L). Asp (D), a polar and negatively charged amino acid, is mutated to Glu (E). Ala (A), a tiny and hydrophobic amino acid, is mutated to Gly (G). The estimated BFE and K_i for each generated complex are reported in Table S1 (Supplementary Material). On the basis of the relation $\Delta G_{\text{bind}} = RT \ln(K_i)$ (R – the gas constant = 1.9872 kcal K⁻¹ mol⁻¹), T – the absolute temperature = 300 K), the experimental range of K_i in between 1 μ M and 0.01 nM corresponds to the BFE (ΔG_{bind}) range in between -8.23 and -15.09 kcal mol⁻¹ for inhibited caspase-2 structures. Numerical inspection of the data in Table S1 identified the complexes that have the BFEs inside of this specific range (Table 3). Thus, as far as affinity issue for the receptor is concerned, the order of preferred inhibitors is: VELAD (K_i =0.081 nM) > VDVAD (K_i =0.23 nM) > VEVAD (K_i =3.7 nM) > VDIAD (K_i =4.5 nM) etc.

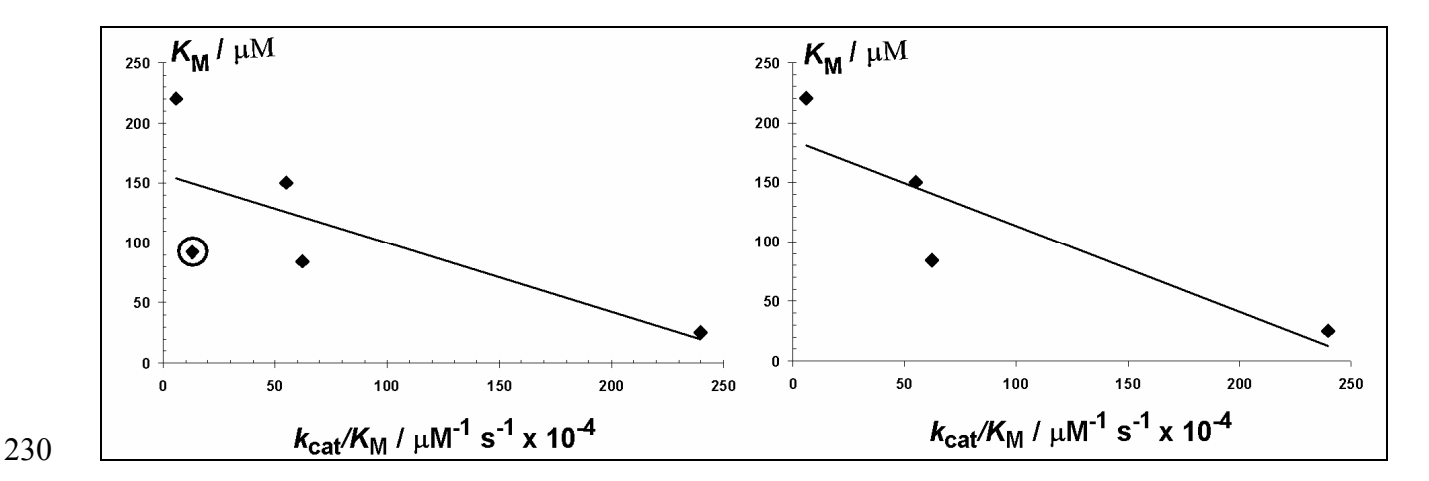


Figure 4. Correlation of the Michaelis constant $(K_{\rm M})$ with the specificity constant $(k_{\rm cat}/K_{\rm M})$ for the experimental caspase-2:peptide structures: $K_{\rm M} = -0.58 \ k_{\rm cat}/K_{\rm M} + 157.51$, R = 0.74 (left). If a data point (denoted by circle, left) is removed, the correlation becomes: $K_{\rm M} = -0.72 \ k_{\rm cat}/K_{\rm M} + 184.99$, R = 0.88 (right).

In order to evaluate the specificity constant for the complexes (Table 3), the correlation of the Michaelis constant with the specificity constant for the experimental caspase-2:peptide structures (Table 1) is observed. Even though two linear correlations are established (Figure 4), the first one ($K_{\rm M} = -0.58~k_{\rm cat}/K_{\rm M} + 157.51$, R = 0.74; Figure 4, left) is slightly more suitable because it reproduces the experimental value of the specificity constant for the caspase-

239 2:VDVAD complex more accurately than the second one (Figure 4, right). Due to the negative 240 slope (-0.58) of the linear regression line, $K_{\rm M} < 157.51~\mu{\rm M}$ represents an approximate condition 241 for the physically meaningful estimate of $k_{\rm cat}/K_{\rm M}$.

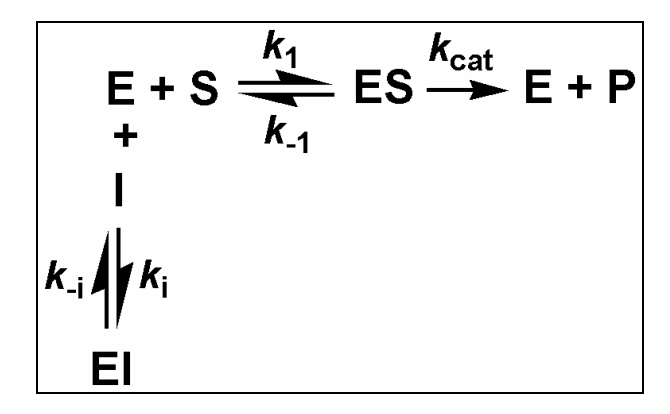


Figure 5. Reaction of competitive inhibition.³⁵

242

244

245

246

251

252

253254

255

256

To evaluate the functional efficiency of the complexes (Table 3) in terms of the specificity constant (k_{cat}/K_M), a competitive inhibition mechanism is considered (Figure 5). For such a reaction, the inhibition constant is defined as:

247
$$K_{i} = \frac{IC_{50}}{(\frac{[S]}{K_{M}} + 1)} = \begin{cases} if [S] = K_{M}, K_{i} = IC_{50}/2 \\ if [S] >> K_{M}, K_{i} << IC_{50} \\ if [S] << K_{M}, K_{i} \cong IC_{50} \end{cases}$$
 (4)

248 where IC_{50} is the inhibitory concentration, $K_{\rm M}$ is the Michaelis constant, and [S] is the substrate concentration. ³⁵ Solving Eq. 4 for the Michaelis constant gives:

250
$$K_{\rm M} = \frac{[S]}{(\frac{IC_{50}}{K_{\rm c}} - 1)}$$
 (5)

The kinetic data are analyzed as follows. IC_{50} is evaluated using its linear correlation with $\Delta G_{\rm bind}$ (Figure 3). $K_{\rm M}$ is evaluated using Eq. 5 with $[S] \approx 2.7$ mM (1 mM = 10^{-3} M) – a typical experimental value. Of these complexes (Table 3), those having $K_{\rm M} < 157.51$ µM are selected (Table 4) and may be considered as competitively inhibited structures. The comparison of the values of $K_{\rm M}$ (Table 4) with respect to [S] shows that $[S] >> K_{\rm M}$, what is in line with $K_{\rm i} << IC_{50}$ according to Eq. 4. The estimate of $k_{\rm cat}/K_{\rm M}$ (Table 4) is made by way of the linear

257 correlation $K_{\rm M} = -0.58~k_{\rm cat}/K_{\rm M} + 157.51$ (Figure 4, left). The specificity constants (Table 4)

indicate that VELAD and VDVAD are most specific to caspase-2, and both are nearly 1.5, 3 and

4 times more specific to the enzyme than VEIAD, VEVAD and VDIAD respectively.

260

261

262

Table 4. Competitive inhibition data for caspase-2:peptide complexes: K_i – inhibition constant, IC_{50} - inhibitory concentration, K_M - Michaelis constant, k_{cat} - catalytic constant, and k_{cat}/K_M - specificity constant

Complex ^(a)	$\Delta G_{\rm bind}$ (kcal mol ⁻¹)	$K_{\rm i} (\mu M)^{(\rm b)}$	IC ₅₀ (nM) ^(b)	$K_{\rm M} (\mu {\rm M})^{(b)}$	$k_{\rm cat}$ (s ⁻¹)	$k_{\rm cat}/K_{\rm M}~(\mu{ m M}^{-1}~{ m s}^{-1})$
casp-2:VELAD	-13.84	0.000081	23.88	9.19	0.24	0.026
casp-2:VDVAD	-13.22	0.00023	25.00	25.00	0.58	0.023
casp-2:VEIAD	-12.64	0.00061	26.15	64.48	1.03	0.016
casp-2:VEVAD	-11.57	0.0037	98.46	105.43	0.94	0.0089
casp-2:VDIAD	-11.45	0.0045	107.69	117.75	0.80	0.0068

263 (a) Ala (A), Asp (D), Glu (E), Ile (I), Leu (L), Val (V)

 $264 \qquad ^{\text{(b)}} 1 \; \mu\text{M} = 10^{\text{-6}} \; \text{M}, \; 1 \; \text{nM} = 10^{\text{-9}} \; \text{M}$

For tightly bound inhibitors, the inhibition constant is:

266
$$K_{i} = \frac{(IC_{50} - [E]/2)}{(\frac{[S]}{K_{M}} + 1)}$$
 (6)

where [*E*] is the enzyme concentration.³⁵ Consequently, the Michaelis constant for tightly bound inhibitors is:

269
$$K_{\rm M} = \frac{[S]}{(\frac{IC_{50} - [E]/2}{K_{\rm i}} - 1)}$$
 (7)

The condition $K_{\rm M}$ < 157.51 μM for tightly bound peptides means:

271
$$\frac{[S]}{(\frac{IC_{50} - [E]/2}{K_i} - 1)} < 157.51 \,\mu\text{M}$$
 (8)

272 Therefore,

273
$$\frac{IC_{50} - [E]/2}{K_{i}} - 1 > \frac{[S]}{157.51}$$
 (9)

Solving Eq. 9 for IC_{50} gives:

275
$$IC_{50} > \frac{[S]}{157.51} K_i + [E]/2$$
 (10)

- For $[S] \approx 2.7$ mM and $[E] \approx 50$ nM typical experimental values, ¹⁰ Eq. 10 gives an approximate 276 condition, IC_{50} (nM) > 17.14 K_i (nM) + 25, which should be satisfied by the tight binding of 277 278 penta-peptides to caspase-2. The values of IC_{50} and K_i (Table 4) indicate that VEVAD and 279 VDIAD satisfy this condition. By reducing [E] from 50 to 44.8 nM, the condition becomes IC_{50} $(nM) > 17.14 K_i (nM) + 22.4$ and is satisfied by VELAD, VEVAD and VDIAD. If [E] is 280 additionally lowered to 42 nM then the condition gets IC_{50} (nM) > 17.14 K_i (nM) + 21, 281 282 indicating that VELAD, VDVAD, VEVAD and VDIAD may be considered as tightly bound 283 inhibitors.
 - The fact that caspase inhibition-based drug has not been approved on the market so far means that the development of therapeutic approaches that specifically target caspases is a substantial challenge of particular biological and clinical interest.³⁶ The present study contributes to the research progress in this field.

4. Conclusions

284

285

286287

288

289

290

291

292

293

294

295

QM/MM model derived and exploited in this work has been shown to correlate with the existing experimental observations to an appreciable extent. This approach has enabled the extensive and systematic investigations of some of the important aspects both of the thermodynamics and of the kinetics of caspase-2 recognition by a large number of pentapeptides. It has been demonstrated that a well-calibrated computational work may yield information inaccessible by other methods or suggest new experimental procedures.

Acknowledgment

- 296 Prof. David A. Case of Rutgers University is acknowledged for granting the author an academic
- 297 license for using the molecular dynamics software package Amber11 in combination with
- 298 AmberTools 1.5.

- 299 Supplementary Material: QM/MM binding free energies for all studied caspase-2:peptide
- 300 complexes are available.
- 301 References
- 1. D. R. McIlwain, T. Berger, T. W. Mak, Cold Spring Harb. Perspect. Biol. 2013, 5, a008656.
- 303 **DOI**:10.1101/cshperspect.a008656
- 304 2. S. Nagata, Annu. Rev. Immunol. 2018, 36, 489-517.
- 305 **DOI**:10.1146/annurev-immunol-042617-053010
- 306 3. G. Krumschnabel, B. Sohm, F. Bock, C. Manzl, A. Villunger, Cell Death Differ. 2009, 16,
- 307 195-207. **DOI**:10.1038/cdd.2008.170
- 4. L. Bergeron, G. I. Perez, G. Macdonald, L. Shi, Y. Sun, A. Jurisicova, S. Varmuza, K. E.
- Latham, J. A. Flaws, J. C. Salter, H. Hara, M. A. Moskowitz, E. Li, A. Greenberg, J. L. Tilly, J.
- 310 Yuan, Genes Dev. 1998, 12, 1304-1314.
- 311 5. L. Bouchier-Hayes, *J. Cell. Mol. Med.* **2010**, *14*, 1212-1224.
- 312 **DOI**:10.1111/j.1582-4934.2010.01037.x
- 313 6. S. Kumar, *Nat. Rev. Cancer* **2009**, *9*, 897-903. **DOI**:10.1038/nrc2745
- 7. H. Vakifahmetoglu-Norberg, B. Zhivotovsky, Trends Cell Biol. 2010, 20, 150-159.
- 315 **DOI**:10.1016/j.tcb.2009.12.006
- 316 8. S. Shimohama, H. Tanino, S. Fujimoto, *Biochem. Biophys. Res. Commun.* **1999**, *256*, 381-384.
- 317 **DOI**:10.1006/bbrc.1999.0344
- 9. J. Y. Kim, R. Garcia-Carbonell, S. Yamachika, P. Zhao, D. Dhar, R. Loomba, R. J. Kaufman,
- 319 A. R. Saltiel, M. Karin, *Cell* **2018**, 75(1), 133-145.e15. **DOI**:10.1016/j.cell.2018.08.020
- 320 10. Y. Tang, J. A. Wells, M. R. Arkin, J. Biol. Chem. 2011, 286(39), 34147-34154.
- 321 **DOI**:10.1074/jbc.M111.247627

- 322 11. PyMol, Version 0.99, W. L. DeLano, DeLano Scientific LLC, South San Francisco CA,
- **2006**.
- 12. D. A. Case, T. Cheatham, T. Darden, H. Gohlke, R. Luo, K. M. Jr. Merz, A. Onufriev, C.
- 325 Simmerling, B. Wang, R. Woods, J. Comput. Chem. 2005, 26, 1668-1688.
- 326 **DOI**:10.1002/jcc.20290
- 13. Amber 11, D. A. Case, T. A. Darden, T. E. Cheatham III, C. L. Simmerling, J. Wang, R. E.
- Duke, R. Luo, R. C. Walker, W. Zhang, K. M. Merz, B. P. Roberts, B. Wang, S. Hayik, A.
- Roitberg, G. Seabra, I. Kolossváry, K. F. Wong, F. Paesani, J. Vanicek, J. Liu, X. Wu, S. R.
- Brozell, T. Steinbrecher, H. Gohlke, Q. Cai, X. Ye, J. Wang, M. J. Hsieh, G. Cui, D. R. Roe, D.
- H. Mathews, M. G. Seetin, C. Sagui, V. Babin, T. Luchko, S. Gusarov, A. Kovalenko, and P. A.
- Kollman, University of California, San Francisco CA. 2010.
- 14. V. Hornak, R. Abei, A. Okur, B. Strockbine, A. Roitberg, C. Simmerling, *Proteins* **2006**, *65*,
- 334 712-725. **DOI**:10.1002/prot.21123
- 15. Gaussian 98, Revision A.9, M. J. Frisch, G. W. Trucks, H. B. Schlegel, G. E. Scuseria, M. A.
- Robb, J. R. Cheeseman, V. G. Zakrzewski, J. A. Montgomery, R. E. Stratmann, J. C. Burant, S.
- Dapprich, J. M. Millam, A. D. Daniels, K. N. Kudin, M. C. Strain, O. Farkas, J. Tomasi, V.
- Barone, M. Cossi, R. Cammi, B. Mennucci, C. Pomelli, C. Adamo, S. Clifford, J. Ochterski, G.
- A. Petersson, P. Y. Ayala, Q. Cui, K. Morokuma, D. K. Malick, A. D. Rabuck, K. Raghavachari,
- J. B. Foresman, J. Cioslowski, J. V. Ortiz, A. G. Baboul, B. Stefanov, G. Liu, A. Liashenko, P.
- Piskorz, I. Komaromi, R. Gomperts, R. L. Martin, D. J. Fox, T. A. Keith, M. A. Al-Laham, C. Y.
- Peng, A. Nanayakkara, M. Challacombe, P. M. W. Gill, B. Johnson, W. Chen, M. W. Wong, J.
- 343 L. Andres, C. Gonzalez, M. Head-Gordon, E. S. Replogle, and J. A. Pople, Gaussian, Inc.,
- 344 Pittsburgh PA, **1998**.
- 345 16. C. I. Bayly, P. Cieplak, W. Cornell, P. A. Kollman, J. Phys Chem. 1993, 97, 10269-10280.
- **DOI**:10.1021/j100142a004
- 17. J. Wang, R. M. Wolf, J. W. Caldwell, P. A. Kollman, D. A. Case, J. Comput. Chem. 2004,
- 348 25, 1157-1174. **DOI**:10.1002/jcc.20035

- 349 18. M. Elstner, D. Porezag, G. Jungnickel, J. Elsner, M. Haugk, T. Frauenheim, S Suhai, G.
- 350 Seifert, *Phys. Rev. B* **1998**, *58*, 7260-7268. **DOI**:10.1103/PhysRevB.58.7260
- 351 19. M. Elstner, P. Hobza, T. Frauenheim, S. Suhai, E. Kaxiras, J. Chem. Phys. **2001**, 114, 5149-
- 352 5155. **DOI**:10.1063/1.1329889
- 353 20. S. Grimme, J. Antony, T. Schwabe, C. Muck-Lichtenfeld, Org. Biomol. Chem. 2007, 5, 741-
- 354 758. **DOI**:10.1039/B615319B
- 355 21. G. M. Seabre, R. C. Walker, M. Elstner, D. A. Case, A. E. Roitberg, J. Phys. Chem. A 2007,
- 356 *111(26)*, 5655-5664. **DOI**:10.1021/jp0700711
- 357 22. R. C. Walker, M. F. Crowley, D. A. Case, J. Comp. Chem. 2008, 29(7), 1019-1031.
- 358 **DOI**:10.1002/jcc.20857
- 359 23. T. Kubar, P. Jurecka, J. Cerny, J. Rezac, M. Otyepka, H. Valdes, P. Hobza, J. Phys. Chem. A
- **2007**, *111*, 5642-5647. **DOI**:10.1021/jp068858j
- 361 24. S. Kristyan, P. Pulay, Chem. Phys. Lett. 1994, 229, 175-180.
- **DOI**:10.1016/0009-2614(94)01027-7
- 363 25. P. Hobza, J. Sponer, T. Reschel, J. Comp. Chem. 1995, 16, 1315-1325.
- 364 **DOI**:10.1002/jcc.540161102
- 365 26. P. Jurecka, J. Sponer, J. Cerny, P. Hobza, *Phys. Chem. Chem. Phys.* **2006**, *8*, 1985-1993.
- 366 **DOI**:10.1039/B600027D
- 367 27. P. Jurecka, J. Cerny, P. Hobza, D. R. Salahub, J. Comp. Chem. 2007, 28, 555-569.
- 368 **DOI**:10.1002/jcc.20570
- 369 28. A. Pavlov, P. M. Mitrasinovic, Curr. Org. Chem. 2010, 14, 129-138.
- **DOI**:10.2174/138527210790069866
- 371 29. P. M. Mitrasinovic, Curr. Drug Targ. 2013, 14, 817-829.
- **DOI**:10.2174/1389450111314070009

- 373 30. P. M. Mitrasinovic, Med. Chem. 2014, 10, 46-58.
- **374 DOI**:10.2174/157340641001131226122124
- 375 31. P. M. Mitrasinovic, Med. Chem. 2014, 10, 252-270.
- **DOI**:10.2174/157340641003140304143442
- 32. P. M. Mitrasinovic, Can. J. Chem. 2003, 81, 542-554. DOI:10.1139/V03-043
- 378 33. P. M. Mitrasinovic, Curr. Org. Chem. 2010, 14, 198-211.
- **DOI**:10.2174/138527210790069857
- 380 34. M. Garcia-Calvo, E. P. Peterson, B. Leiting, R. Rue, D. W. Nicholsoni, N. A. Thornberry, J.
- 381 *Biol. Chem.* **1998**, *273(49)*, 32608–32613. **DOI**:10.1074/jbc.273.49.32608
- 382 35. R. Z. Cer, U. Mudunuri, R. Stephens, F. J. Lebeda, *Nucl. Acids Res.* **2009**, *37*, W441-W445.
- 383 **DOI**:10.1093/nar/gkp253
- 384 36. J. Kudelova, J. Fleischmannova, E. Adamova, E. Matalova, J. Physiol. Pharmacol. 2015,
- 385 *66(4)*, 473-482.